Fatigue Crack Growth in Thin-Wall Pipes Subjected to Bending

Mohammad Mahdi Amiri *
Department of Engineering,
Research Institute of Petroleum Industry
E-mail: amirimm@ripi.ir
*Corresponding author

Received: 22 December 2018, Revised: 22 February 2019, Accepted: 10 May 2019

Abstract: In this paper, a circumferential external surface flaw in a metallic round pipe under cyclic bending loading is considered. Because of very rapid changes in the geometrical parameters around the crack front region, the mesh generation of this region must be done with great care. The analysis of the fatigue crack growth is done in accordance with Paris law. The spread lane of the exterior defect is achieved from the graph of "α" vs. "relative crack depth". The growth of fatigue crack is also analyzed (the comparative crack depth against loading runs diagram) with various initial crack "α" beneath periodic loading. Fatigue shape growth of primarily semi-elliptical peripheral surface flaws is shown. The weight of the Paris exponent (material constant) on fatigue crack propagation is presented as well. Furthermore, the "fatigue crack growth" progression of several specimens is evaluated experimentally by employing a manually-constructed experimental setup. Conclusively, the experimental results achieved by periodic bending loading tests are compared with the numerical results. Fatigue shape development of initially semi-elliptical external surface defects is illustrated. The effect of the Paris exponent (material constant) on fatigue crack propagation is shown as well. Moreover, the fatigue crack growth of several specimens is assessed experimentally using a manually-constructed experimental set up. Finally, the experimental results obtained by cyclic bending loading tests are compared.

Keywords: Fatigue Crack Growth, K (Stress Intensity Factor), Semi-Elliptical Crack, Thin-Wall Pipes

Reference: Amiri, M. M., "Fatigue Crack Growth in Thin-Wall Pipes Subjected to Bending", Int J of Advanced Design and Manufacturing Technology, Vol. 12/No. 2, 2019, pp. 83–90.

Biographical notes: Mohammad Mahdi Amiri received his PhD in Mechanical Engineering from Sharif Technology Development Institute 2017. He has previously obtained his BSc and MSc from K. N. Toosi University of Industry. He is currently a member of the scientific board of Research Institute of Petroleum Industry (RIPI). His current research interest includes Pressure Vessels and Piping, Solid Mechanics and Oil and Gas industry.

© 2019 IAU, Majlesi Branch

1 INTRODUCTION

Propagation of a semi-elliptical crack is mostly understood on the surface of the defect in some constructions like cylinders, bolts, reactors, pressure vessels, etc. A pipeline stress analysis is an important part to design it but it is not sufficient. In addition to stress analysis, span analysis is another issue for designing. It is important to calculate it correctly in order to have a good and safety design of the pipeline. In span analysis the following items should be considered:

- Excessive yielding
- Fatigue
- Interface with human activity

There are several reasons to induce fatigue failure of a pipe such as preventing crack growth and so on. The fatigue is created in a pipe mostly deals with corrosion fatigue and resonance fatigue. Therefore, for designing a pipe to protect it against the mentioned fatigue a using proper material in the coating is essential. There are some solutions to solve the problem caused by two different fatigues. For example, if the problem is related to resonance fatigue in pipeline traditionally, using a simple model to evaluate the potential of a span to undergo resonance is based on comparison of shedding frequency and natural frequency of the span. According to researches, pipeline rested on the seabed are subjected to fluid loading from both waves and steady currents. So, it is a design requirement that the pipe should be sufficient to ensure stability. In most case, a concrete weight coating on pipeline provides this weight.

Several researchers have studied that the fatigue propagation of external flaws in steel pipes is clearly affected by the shape of the flaw, which differs for any type of loading. Shahani and Habibi [1] measured the drawback of mixed mode rupture brought by a semi-elliptical peripheral crack lying at the exterior side of the cross-section of a hollow pipe. The pipe was beneath effective axial forces, torsion and bending moment. The performance of semi-elliptical surface cracks in plates, pipes and rods was investigated by numerous researchers (Lin and Smith [2], Underwood [3], Raju and Newman [4], Couroneau and Royer [5], Carpinteri and Brighenti [6] and Pook [7]). A wide-ranging list of references is stated in Shahani and Habibi [1]. Conversely, only a few analyses have been completed on peripheral surface defects in cylinders (Carpinteri et al. [8], Bergman [9] and Peng et al. [10]). There is an approximate technique, namely the line spring method, for computing the SIFs aiming the simplification of the problem.

Today, with the aid of new numerical tools, it is possible to analyze very complex geometry and loading conditions in a relatively short time. One of these advanced techniques is the sub-modeling technique. The method is also called the cut-boundary displacement method or the specified boundary displacement method. The submodeling method is based on the Saint-Venant's principle, that is, if actually the distributed boundary traction is replaced by the statically equivalent boundary condition, the solutions of elasticity are only altered near the boundary where the equivalent boundary condition is prescribed, and for the point which is relatively far from the cut boundary, the solution is not affected. If the boundary of the submodel is reasonably selected, and a fine mesh is used for the sub-model, then high-accuracy results can be achieved. At first, the structure being analyzed is modeled through a coarse mesh. Then, the region of interest, which needs very dense mesh, is cut from the whole model and is analyzed with high density mesh.

In analyzing the submodel, the displacement boundary conditions are extracted from the whole model and applied on the cutting boundary of the sub-model. In the present paper, a circumferential external surface flaw in a metallic round pipe under cyclic bending loading was considered ("Fig. 1"). A three-dimensional finite element analysis is carried out to calculate the stress intensity factor distribution along the crack front. Because of very rapid changes in the geometrical parameters around the crack front region, mesh generation of this region must be done with great care. This may lead to an increase in run time which makes it difficult to reach valid results and conclusions. To overcome the above mentioned disadvantage, the sub-modeling technique is used. Then, using the Paris equation, the fatigue crack growth is modeled for any points of the crack front to reach the new shape of the crack at each step. The propagation path of fatigue crack growth is studied. Then, some experiments have been conducted using a manually designed and fabricated experimental set up for combined fatigue loading tests. Comparison of the finite element (FE) results with the experimental results shows a good agreement between them.

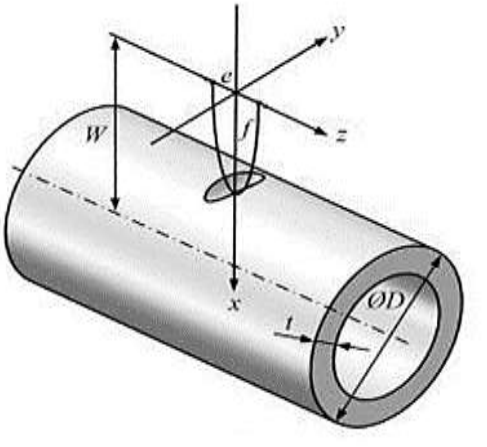

Fig. 1 Common circumstances of the problem.

© 2019 IAU, Majlesi Branch

2 FEM ANALYSIS

In "Fig. 2" the rounded cross-section of a pipe with a peripheral semi-elliptical flaw, which its center is set on the exterior side of the cross-section, is presented.

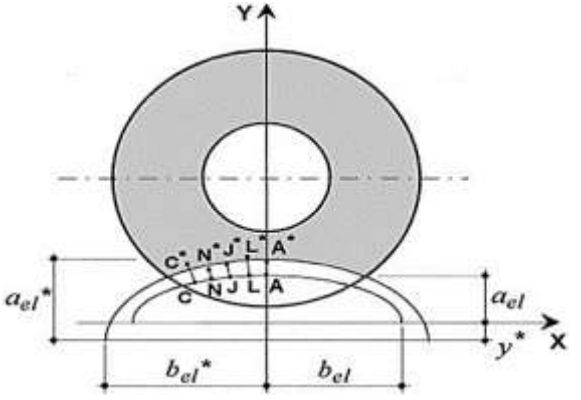

Fig. 2 Cross-section of the cylinder.

The geometry of this crack can be displayed by two dimensionless factors, α = a/c and ξ = a/t, the supposed "aspect ratio" and "relative depth" of the crack, respectively. Any peripheral point on the flaw face can be expressed by a dimensionless coordinate considered as 'normalized coordinate', ξas below:

$$\xi = \frac{X_P}{X_G} \tag{1}$$

Respectively X_P and $X_G$are the X-coordinate of the point P and the corner point G, ("Fig. 2"). Per couple of supposed values for $\xi$and α, the K (stress intensity factor) in mode I condition (K_I) could be found as a displacements function, which is shown as below: [1]:

$$\mathrm{K_I} = \frac{2\mathrm{G}}{(1+\mathrm{K})}\left(\frac{2\pi}{\mathrm{a}}\right)^{\frac{1}{2}}\mathrm{U_y} \tag{2}$$

With

$$\mathrm{K} = \begin{cases} \dfrac{3-\nu}{1-\nu}\,; \text{Plane stress} \\ 3-4\nu\,; \text{Plane strain} \end{cases} \tag{3}$$

As E and G are the shear modulus and Young's modulus, ν is the Poisson's ratio, Uy is the dislocation in the y direction and so a is the length of the crack. Because of the benefits of using dimensionless analysis, this lemma is used here, and the factors of stress intensity are made normal in accordance with the next correlation:

$$\mathrm{K_{non}} = \frac{\mathrm{K_{cal}}}{\mathrm{K_0}} \tag{4}$$

Where K_{cal} is the calculated value of the K (stress intensity factor) and $K_0 = \sigma\sqrt{\pi a}$ is the nominal K because of axial stress, σ.

The lanes of fatigue growth in the peripheral surface crack in the cylinder are obtained in the graph of α versus ξ with the use of two-parameter model theory (unchanging ellipse center on the exterior side of the cylinder) based on Paris law:

$$\frac{da}{dN} = C(\Delta K)^n \tag{5}$$

Where N is the number of loading cycles and $\frac{da}{dN}$ is the rate of crack growth in $\frac{mm}{cycle}$ and ΔK is the periodic K in MPa$\sqrt{mm}$.

Furthermore, the material constants C and n in the Paris law are assumed to be equal to 1.64×10-10 and 2, respectively [8]. Since the new locations of the points on the crack face are pointed in the different time steps, it is seen that the new arrangements are well-fitted with the ellipse equation:

$$\frac{x^2}{a^{*2}} + \frac{y^2}{c^{*2}} = 1 \tag{6}$$

Where a* and c* are the semi-axis lengths of the ellipse.

3 EXPERIMENTAL FABRICATED TESTING MACHIN

Figure 3 represents an invented testing mechanism for employing mixed loading to various specimens. The capability of this device for applying bending moment along with torsion and axial loading parallel and independently is almost unique; nevertheless, the purpose of this paper is to study the effect of bending moment on the growth of the crack. The primary parts of the machine encompass chassis, cam disk (loading mechanism), shear loading mechanism and motor power. The length of the main chassis is 3 meters when loading mechanism is applied by cam disk, shear loading mechanism and motor power are also connected to it. The chassis has sufficient strength to undergo the vibration and tension exerted by the system. "Mixed Fatigue Testing Mechanism" elements are presented in an additional table to the "Fig. 3".

© 2019 IAU, Majlesi Branch

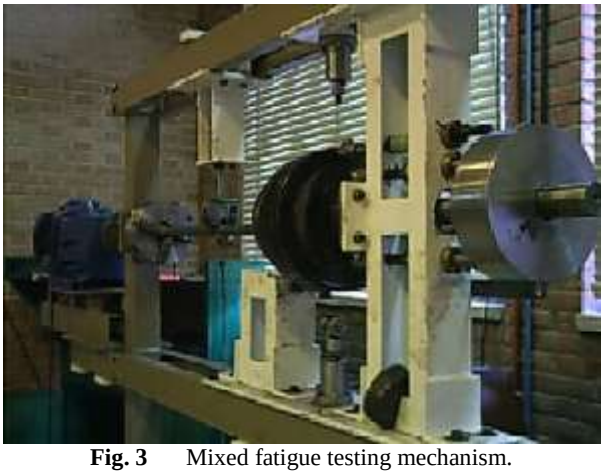

Fig. 3 Mixed fatigue testing mechanism.

The key part of the system for load applying is the cam disk including unique cam profiles on both sides of it ("Fig. 4"). These profiles make applying bending moment together with torsion on the tubular specimen. It is likely to employ rotating bending to the pipe in two modes. First by a spring loaded shaft which could be titled the shear loading mechanism (Part e in "Fig. 3"), and second, by pushrods operating on the cam profiles as presented in "Fig. 4".

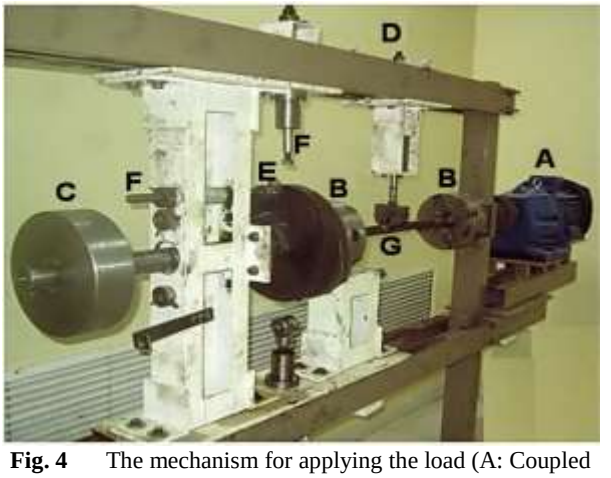

Fig. 4 The mechanism for applying the load (A: Coupled Electric Motor, B: Four Jaw Chuck, C: Balancing Weight, D: Machine Mainframe, E: Cam Disk, F: Loading Device, G: Sample Pipe).

The support that endures the cam disk is flexible enough to balance the required movements for employing the loads. The pair of cam profile and pushrods is also capable of employing repeated axial force on the cylinder or pipe. As mentioned above, in this paper the pure bending moment has been employed to the pipe. The specimens were fine-tuned between jaws of the machine, while from one side it is rotated by an electrical motor via a gearbox and from the other side the load is applied by a cam disk ("Fig. 3").

The main loading part of the system is the cam disk including unique cam profiles on both sides of it ("Fig. 4").

4 FINDINGS AND DISCUSSION

The existence of a free surface effect varies the stress state near the crack face from a 3-dimensional, more closely plane strain, on the interior points to a 2-dimensional one, roughly plane stress state, near the surface points. The district of more plane stress near the surface is more resisting to fatigue crack growth than those regions which are in different directions from the surface. This means that the growth of internal points is more than the corner points. In the first step, for studying the precision of the model, a cracked pipe with α=0.6 and ξ=0.3 is considered. If we change the number of elements, the obtained results could be compared with each other ("Table 1"). In each step of the analysis, the mechanical parameter error in energy norm is considered and the convergence of outcomes is shown.

Table 1 Concerns of precision in sub-model with crack α 0.6 against ξ=0.3

	Total elements	Structural parameter error in the energy norm	No. of singular element	Time (min)
1	1312	6.6277	16	4
2	1800	6.3889	20	6
3	2538	6.272	24	8
4	3074	6.2434	30	12

By comparing the results in "Table 2", it is clear that the increment in the number of elements in the model could increase the required time for analysis. By use of a sub-model, the run time for the program decreases considerably. For instance, with the use of a sub-model with 30 singular elements, the run time lessened about 0.1 compared to the entire model with the same precision and the same number of singular elements. Regarding the condition of reducing differences in the structural parameter error in the energy norm, it could be concluded that the model became independent of elements.

Figure 5 represents the distribution of the K on the flaw face, which is depending on normalized coordinate ξ, for an employed bending moment. The outcomes are considered for various values of the α and a constant relative crack depth of 0.3. As presented in "Fig. 5", for a constant ξ, the reduction of the crack α raises the SIF. It is noteworthy to consider the symmetrical distribution of the SIF. Likewise, the results demonstrate a transition of the maximum SIF from the lowest point of the cracks (z=0) to the corner points (z=1), for an α value which is

© 2019 IAU, Majlesi Branch

equivalent to about 1.0, a result which shows acceptable agreement with [1].

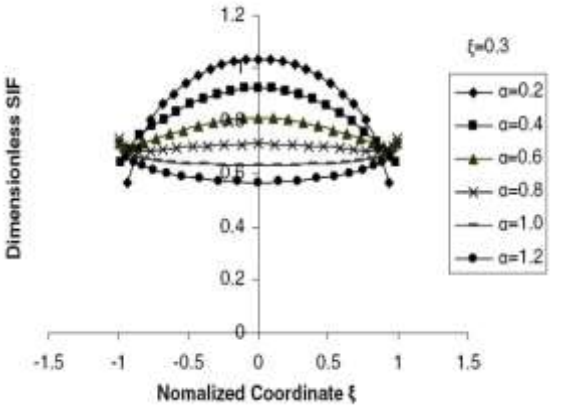

Fig. 5 "K" on the face of crack as a function of the normalized coordinate of points in a case of bending moment (ξ=0.3).

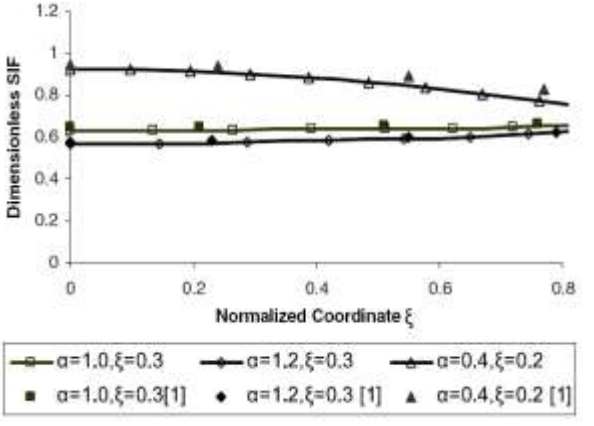

Fig. 6 The results of our study compared with the others [1].

The distribution of "K" on the crack face for various values of aspect ratios and relative depths are shown in the "Table 2".

Table 2 Dimensionless maximum stress intensity factor K_{max}, at different points (A, B, C, D and E) on the crack front

$R^* = \frac{R2}{t} = 10$			$\xi = \frac{a}{t}$						
$\alpha = \frac{a}{c} =$		0.1	0.2	0.3	0.4	0.5	0.6	0.7	0.8
0.2	A=0	.923	1.07	1.11	1.18	1.20	1.23	1.27	1.26
	B=0.28	.900	1.04	1.08	1.15	1.18	1.22	1.26	1.28
	C=0.55	.879	.987	1.01	1.05	1.10	1.12	1.20	1.25
	D=0.76	.826	.854	.878	.900	.958	1.02	1.08	1.15
	E=0.96	.670	.383	.468	.529	.766	.770	.781	.987
0.4	A=0	.868	.946	.889	.950	.985	1.00	1.02	1.02
	B=0.24	.853	.936	.882	.945	.978	.998	1.02	1.03
	C=0.55	.801	.890	.843	.923	.944	.974	1.01	1.04
	D=0.77	.755	.827	.799	.876	.893	.921	.979	1.02
	E=0.96	.670	.640	.670	.764	.835	.874	.934	.980
0.6	A=0	.749	.826	.836	.844	.852	.859	.866	.862
	B=0.26	.741	.819	.829	.841	.848	.856	.868	.868
	C=0.52	.720	.798	.810	.824	.835	.836	.870	.885
	D=0.75	.687	.765	.780	.797	.817	.837	.870	.898
	E=0.98	.672	.747	.776	.803	.835	1.02	1.11	.980
0.8	A=0	.683	.725	.733	.745	.754	.765	.772	.769
	B=0.29	.681	.722	.729	.741	.752	.766	.772	.776
	C=0.56	.674	.713	.721	.736	.748	.767	.784	.794
	D=0.79	.665	.702	.715	.737	.752	.776	.801	.821
	E=0.98	.686	.728	.745	.781	.810	.850	.895	.928
1	A=0	.589	.619	.651	.659	.663	.667	.668	.665
	B=0.21	.590	.621	.651	.660	.665	.669	.672	.670
	C=0.51	.598	.630	.656	.666	.673	.680	.688	.692
	D=0.76	.611	.645	.666	.678	.689	.702	.716	.728
	E=0.98	.665	.704	.727	.748	.771	.780	.833	.864
1.2	A=0	.530	.553	.578	.587	.711	.592	.594	.591
	B=0.23	.535	.558	.582	.685	.717	.597	.599	.598
	C=0.55	.555	.580	.599	.647	.744	.619	.626	.629
	D=0.79	.582	.609	.625	.617	.785	.654	.665	.674
	E=0.99	.649	.680	.697	.588	.909	.757	.783	.807

© 2019 IAU, Majlesi Branch

In order to validate the results, a comparison is done with those of reference [1], as given in "Fig. 6" very good consensus is seen. Frequently, two different situations for fatigue crack growth are available for pipes, which are under loading.

In the first one, all propagation ways for $\alpha \geq 0.2$ incline to converge horizontally asymptotic $\alpha=1$ so quickly, i.e., the face of such cracks turn out to be circular arc-shaped. Instead, for $\alpha \leq 0.2$, the crack α grows so gradually throughout the fatigue crack growth ("Fig. 7").

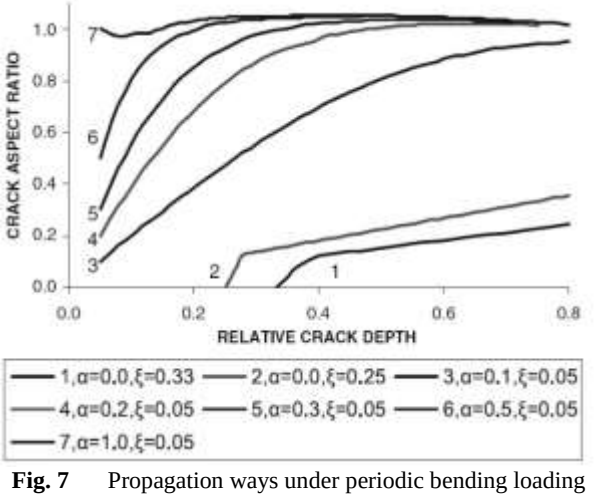

Fig. 7 Propagation ways under periodic bending loading in various primary crack patterns.

In order to validate the results, a comparison should have been done between the gained results and those of reference [8] and a relatively good consensus is seen ("Fig. 8").

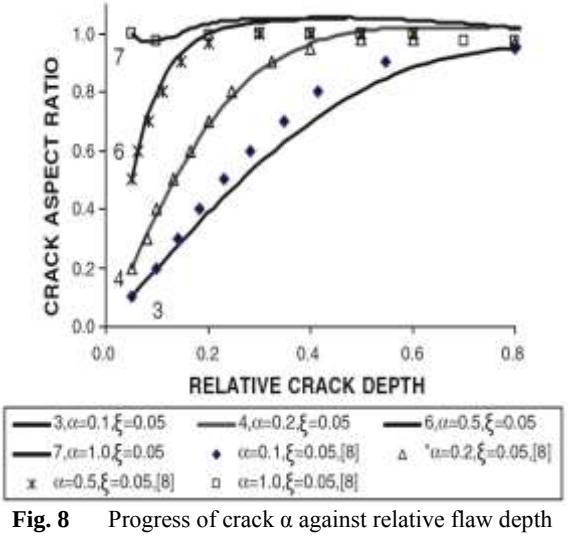

Fig. 8 Progress of crack α against relative flaw depth under cyclical bending loading.

The juncture angle of the flaw corner point with the exterior surface of the cylinder (β) throughout crack growth is plotted versus the parameter ξ in "Fig. 9" for the first seven original crack arrangements. As could be clearly seen in "Fig. 9", the intersection angle, which is gained for thin-walled cylinders numerically under cyclical bending, inclines to 90° as the crack deepens.

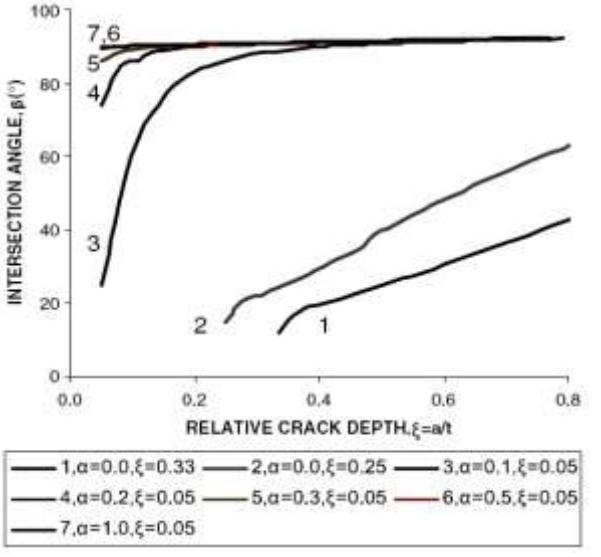

Fig. 9 The intersection of crack face angle β, versus the depth of the relative crack.

Figure 10 represents the relative crack depth against the number of cyclical loading (which was divided by 108), for the surface cracks. Four various estimates are compared in the "Fig. 10". It is shown that how the α of the pre-crack becomes lower, the crack growth rate will become higher. Instead, a definite length of the crack is gained for a lower initial α crack at lower cycles of load.

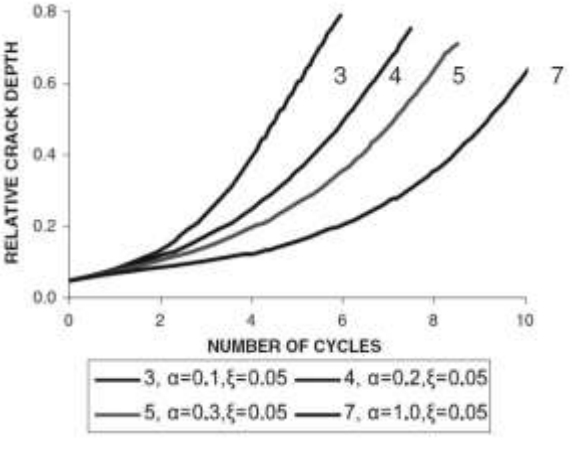

Fig. 10 The ξ of crack versus the number of cyclical loads (multiplied by 10^{-8}).

Figure 11 demonstrates the development of fatigue shape of semi-elliptical surface crack under cyclical bending. The crack profiles shown in "Fig. 11" are those

© 2019 IAU, Majlesi Branch

reduced from a range of 80~100 studies for each failure, with the purpose of gaining meaningful outcome.

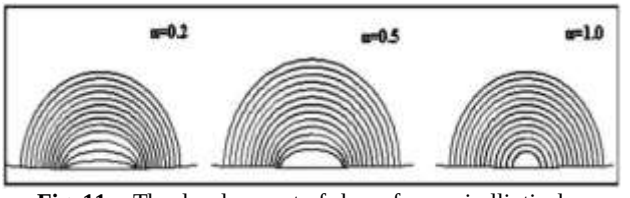

Fig. 11 The development of shape for semi-elliptical surface cracks under bending.

There are 3 different kinds of aspect ratios, i.e., 0.2, 0.5 and 1 which were studies. It is noteworthy that all of these cracks develop into the shape of a semi-circular crack after a few cycles. Mostly, the ending profile, that a flaw will accept, is contingent on its primary α, but if the original α which is equal to a_0/c_0 is not so little and the original ξ which is equal to a_0/t, is not so huge, an approximately constant ending shape would not be available. A study on the effect of Paris equation factor (n), on the different α has been done by choosing three different exponents, n=2, 3 and 4, in order to make a model of originally semi-elliptical surface crack (α_0=0.1 and ξ_0=0.05) under bending. The outcomes are given in "Fig. 12", which implies that the effect of *n* on the α is obvious and a greater *n* makes the α deviation more severe.

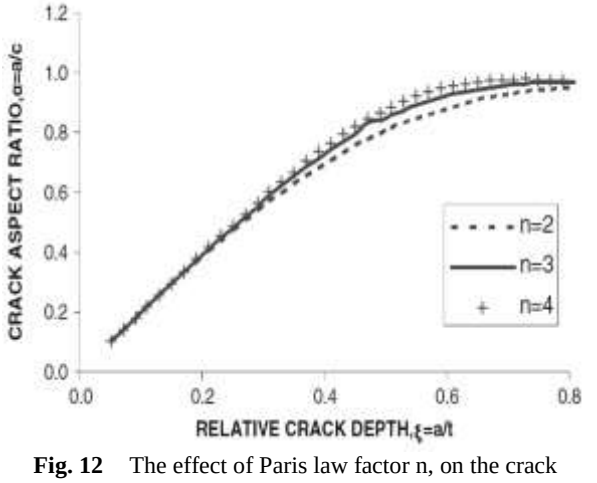

Fig. 12 The effect of Paris law factor n, on the crack growth in a pipe subjected to cyclic bending.

Figure 13(a) shows a common sample with a primary straight crack face after the fracture. All the pre-cracks were made with a thin wire cut machine and so had a straight front. It is clear that the shape of crack changed into a semi-elliptical.

Regarding crack growth in mode I, the cross section of the cylinder following failure is bright, flat and equivalent with the primary crack plane as is observed from "Fig. 13(b)". Conclusively, the outcomes gained from experiments were compared with numerical analysis outcomes ("Fig. 14"). The α of the pre-cracks with a straight crack face is α=0. Six samples containing cracks with different ξ were chosen from the experiments and the "α" of them and also their "ξ" at the breakdown ("Table 3") were compared with the results from FE analysis ("Fig. 14").

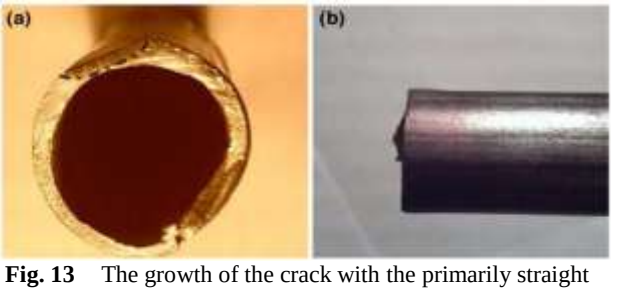

Fig. 13 The growth of the crack with the primarily straight crack front in a cylinder subjected to bending: (a): primary and ending shapes of the crack and (b): the cylinder side view.

Table 3 Investigational outcomes for the "fatigue growth" of the superficial flaws

Specimen	t	a_0	c_0	$\alpha_0 = \frac{a_0}{c_0}$	$\zeta_0 = \frac{a_0}{t_0}$	$\alpha = \frac{a}{c}$	$\zeta = \frac{a}{t}$
a	4	1	-	0	0.25	0.36	0.99
b	4	1	-	0	0.25	0.46	0.88
c	3	1	-	0	0.33	0.45	0.9
d	3	1	-	0	0.33	0.42	0.8
e	3	2	-	0	0.67	0.47	0.91
f	3	2	-	0	0.67	0.31	0.96

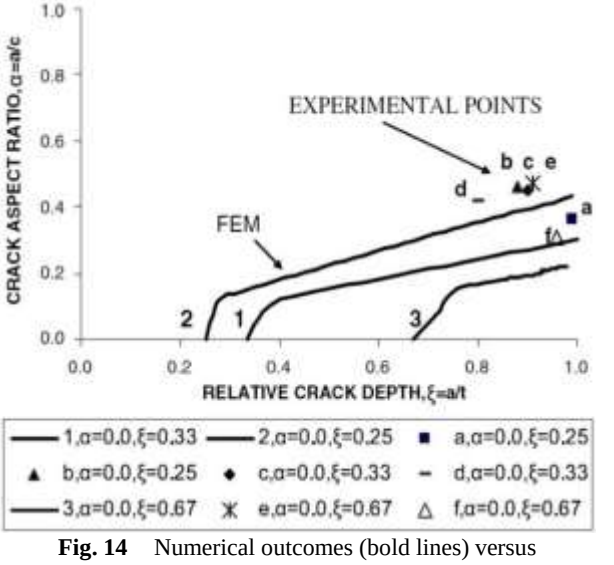

Fig. 14 Numerical outcomes (bold lines) versus experimental outcomes.

Acceptable compliance is witnessed between the results. The investigational outcome concerning a complete fatigue test on a cylinder containing a crack entitles just

© 2019 IAU, Majlesi Branch

one point on the graph. Our limitations in measuring a crack dimension before a complete fracture compel us to measure the crack size only after the full breakdown of the pipe. Nonetheless, the FE analysis foretells all the crack growth steps from the preliminary dimensions to the ending shape of the crack ("Fig. 14"). This implies the efficiency of the FE model which was done in an accompanying research.

5 CONCLUSION

The performance of a semi-elliptical peripheral crack in a steel rounded cylinder under cyclical bending loading has been studied and also some experimental tests through the use of an invented mixed fatigue-test mechanism were managed. The subsequent conclusions could be drawn:

– A delinquent which is faced in the 3-dimensional FE analysis is the considering number of elements and as a consequence, a significant and time-consuming calculation. To overcome this drawback, the sub-modelling technique is applied.
– A certain value for the α exists, under which the maximum K befalls at the deepest point of the flaw. Nonetheless, for aspect ratios more than this value the maximum "K" is shifted to the points on the corner. This certain value may be regarded as "transition aspect ratio".
– The sequence of stress singularity at the points on the corner of the semi-elliptical crack is different from the familiar square-root singularity, that befalls at other points of the crack face, and is reliant on the junction angle of the crack face curve with the margin of the pipe (β in "Fig. 2"). So, the use of supposed quarter point singular elements that model the square-root singularity returns consistent results at all points along the crack face excluding those that are in the close neighbourhood of the points on the corner.
– Fatigue crack propagation lanes in the graph of "α" versus "relative crack depth" have been determined through a two-parameter model. It can be stated that these ways arrive at the same destination in the horizontal asymptote α=1.0 (circular arc face) so quickly for $\alpha 0 \geq 0.2$, as α increases very slowly throughout the "fatigue crack growth" for $\alpha 0 \leq 0.2$.
– The intersection angle β between the crack face and peripheral surface tends to 90° as the crack grows.
– A comparison was made between experimental results gained by cyclical bending tests and the numerical outcomes. The consensus between experimental results and the finite element results are satisfactory. Alternatively, since the crack growth befalls in mode I, the cross section of the cylinder after breakdown is bright, flat, and comparable with the primary crack plane, as predicted.

REFERENCES

[1] Shahani, A. R., Habibi S. E., Stress Intensity Factors in Hollow Cylinder Containing a Circumferential Semi-Elliptical Crack Subjected to Combined Loading, International Journal of Fatigue, Vol. 291, No. 1, 2007, pp. 128–140. doi: 10.1016/j.ijfatigue.2006.01.017.

[2] Lin X. B., Smith, R. A., Fatigue Growth Prediction of Internal Surface Cracks in Pressure Vessels, International Journal od Press Vessel Technology. Vol. 120, No. 1, 1998, pp. 17–23, doi:10.1115/1.2841878.

[3] Underwood J., Stress Intensity Factor for Internally Pressurized Thick-Walled Cylinders: Stress Analysis Growth Cracks, ASTM STP, Vol. 513, 1972, pp. 59–70.

[4] Raju, I. S., Newman, J. C., Stress-Intensity Factor for Internal and External Surface Cracks in Cylindrical Vessels, International Journal of Press Vessel Technology., Vol. 104, No. l, 1982, pp. 293–298.

[5] Couroneau, N., Royer, J., Simplified Model for the Fatigue Growth Analysis of Surface Cracks in Round Bars Under Mode I, International Journal of Fatigue, Vol. 20, No. 10, 2010, pp. 711–718, doi:10.1016/S0142-1123(98)00037-1.

[6] Carpinteri, A., Brighenti R., A Three-Parameter Model for Fatigue Behavior of Circumferential Surface Flaws in Pipes, International Journal of Mechanical Science, Vol. 42, No. 7, 2000, pp. 1255–1269, doi:10.1016/S0020-7403(99)00083-1

[7] Pook, L. P., On Fatigue Crack Paths, International Journal of Fatigue, Vol. 17, No. 1, 1995, pp. 5–13, doi:10.1016/0142-1123(95)93045-4.

[8] Carpinteri, A., Brighenti, R., and Spagnoli, A., Part-Through Cracks in Pipes Under Cyclic Bending, Nuclear Engineering and Design., Vol. 185, No. 1, 1998, pp. 1–10, doi:10.1016/S0029-5493(98)00189-7.

[9] Bergman, M., Stress Intensity Factors for Circumferential Surface Cracks in Pipes, Fatigue & Fracture of Engineering Materials & Structures, Vol. 18, No. 10, 1995, pp. 1155–1172. doi:10.1111/j.1460-2695. 1995.tb00845. x.

[10] Peng. D., Wallbrink, C., and Jones, R., An Assessment of Stress Intensity Factors for Surface Flaws in a Tubular Member, Engineering Fracture Mechanics, Vol. 72, No. 3, 2005, pp. 357–371. doi: 10.1016/j.engfracmech.2004.04.001.

© 2019 IAU, Majlesi Branch